Fourteenth USA/Europe Air Traffic Management Research and Development Seminar (ATM2021)

Modeling of Flight Time Prediction Uncertainty for Four-Dimensional Descent Trajectory Management

Noboru Takeichi and Ryota Hashimoto
Department of Aeronautics and Astronautics
Tokyo Metropolitan University
Hino, Tokyo, JAPAN
takeichi@tmu.ac.jp

***Abstract*—This study presents a model for flight-time prediction uncertainty on descent trajectories. Providing the magnitude of flight-time prediction uncertainty on descent trajectories is expected to enable efficient management of traffic flow towards congested airports without affecting safety. Flight-time prediction uncertainty inevitably increases as a flight progresses, owing to fluctuations of atmospheric conditions and aircraft control. In addition, atmospheric conditions and aircraft ground speed can vary significantly in descent trajectories. To develop a model for flight-time prediction uncertainty on descent trajectories, first a model of the increase in flight-time prediction uncertainty over short trajectory segments is derived theoretically. Its coefficients are determined through clustering and regression analysis of actual flight data and numerical weather forecast data. Then, a theoretical model of flight-time prediction uncertainty over descent trajectories is formulated to enable the calculation of flight-time uncertainty of descent trajectories using the short trajectory segment data. Through analysis of modeling accuracy of flight-time prediction uncertainty over a large number of actual descent trajectories, the proposed method is demonstrated to provide accurate flight-time prediction uncertainty of descent trajectories even under calm and severe conditions.**

Keywords—4D trajectory management; trajectory prediction; uncertainty modeling; descent trajectory

I. INTRODUCTION

As part of a long-term strategy to meet the increasing demand for air transportation, civil aviation authorities are planning to introduce time-based operations into future air-traffic management systems [1,2]. Accurate and reliable prediction of estimated time of arrival (ETA) is believed to improve the safety and efficiency of air-traffic management [3]. Applications of model of flight-time prediction uncertainty have been investigated, such as displaying ETA uncertainty on the monitors of air traffic controllers (ATCOs) and pilots [4–6]. Achieving specific ETA accuracy will ensure the safety of time-based merging at a particular waypoint (WP) and of landing at congested airports [7–9]. The ETA accuracy is also understood as a key metric for evaluating the performance of the time-based flow management [10] and for ensuring safe and efficient separation on final approach [11]. Operational time uncertainty is correlated with several factors, such as departure time uncertainty; weather forecast errors; and tracking, navigation, and control errors. Among these, this study focuses on the flight-time prediction uncertainty caused by atmospheric fluctuations and aircraft control errors.

In previous studies on ETA uncertainty, it was theoretically proven that the standard deviation (STD) of positional variability is proportional to the flight distance or time [3,12], and this was later confirmed by data analysis [13–16]. The relationship with atmospheric conditions was focused on and the uncertainty of wind speed was taken into account using ensemble weather forecasting. Studies have been conducted on estimating trajectory uncertainty [17], robust and efficient trajectory planning [18,19], and estimating uncertainties in fuel consumption [20]. Recently, the variability of flight speed–a source of ETA error in on-board flight time prediction–has been modeled for level trajectories using forecast values of wind speed and temperature based on uncertainty propagation theory and actual data analysis [21], and an improved model for flight time prediction uncertainty at arbitrary distances has been developed [22]. In addition, machine learning techniques have also been applied to predict ETA and its uncertainty using various influential factors including atmospheric conditions and traffic conditions that may be difficult to model analytically [11, 23, 24]. A flight time prediction uncertainty model considering atmospheric conditions will assist ATCOs in ensuring safety by maintaining a larger time-based separation during severe weather conditions, and will improve operational efficiency by reducing separation to the minimum necessary for safety during calm weather conditions. In this way, an accurate model of flight time prediction uncertainty will allow ATCOs to reduce potential deficiencies in both safety and efficiency.

As mentioned above, the time-based air-traffic management will be applied to congested airports. With this, it is conceivable that flights will merge at one WP in the vicinity of an airport after descent. Therefore, the model of flight-time prediction uncertainty of each flight before descent is beneficial for safe and efficient operations at congested airports. Since existing methods [21,22] are based on uncertainty propagation theory, they have an advantage that machine learning can never achieve: they provide exact mechanisms between uncertainty and atmospheric and flight conditions using necessary and sufficient parameters. However, since the wind speed and temperature vary gradually over descent trajectories, the existing methods cannot be directly applied. In order that the flight-time prediction uncertainty at the merging point of each descent flight will be provided for the ATCOs based on detailed weather forecast information, this study presents a new modeling method extending the existing one [21] so that it can

take into account the variation of flight and atmospheric conditions.

II. Data for Analysis

In this study, a series of flight data acquired from the experimental Secondary Surveillance Radar mode S radar sites in Tokyo and Sendai in Japan for the years of 2017 and 2018 are examined. These data include the aircraft type, indicated airspeed (IAS), true airspeed (TAS), ground speed (GS), Mach number, pressure altitude, azimuth angle, and true track angle recorded every 10 s [25]. For the weather forecast data, the Meso-Scale Model (MSM) of numerical forecast data [26] is employed. The MSM data are updated every 3 h and provide the forecast temperature and wind information every 3 h for the next 39 h at grid points placed every 0.1° in longitude and 0.125° in latitude at pressure altitudes of every 50–100 hPa. In the analysis, the forecast values are calculated using linear interpolation on time, longitude, latitude, and pressure using the latest forecast data.

Aircraft on descent trajectories are usually controlled to maintain the IAS below the transition altitude, track angle, and sink rate or flight path angle (FPA). Therefore, only the flight trajectories that continuously satisfy the following conditions for more than 20 km are extracted as the controlled ones: initial altitude below 35,000 ft and above 10,000 ft, mean sink rate smaller than −500 ft/min, true track angle of 30–150°, and maintaining IAS within 10 kt, true track angle within 5°, and sink rate within 500 ft/min or FPA within 0.5°. Thus, 80,543 trajectories are extracted. The horizontal and vertical trajectories are shown in Fig. 1. Of these, 1108 have a total length exceeding 100 km. In this study, the feasibility of the flight time uncertainty prediction is evaluated using the 1108 trajectories. The vertical trajectories of 100 example trajectories and their histories of pressure altitude, GS, tailwind, crosswind and temperature are shown in Fig. 2. Histograms of the initial pressure altitude and mean IAS of the 1108 trajectories are shown in Fig. 3. It can be observed that the flight and atmospheric conditions gradually change with the descent. The focus of this study is modeling the uncertainty of flight time prediction error of aircraft with such continuous changes in flight and atmospheric conditions.

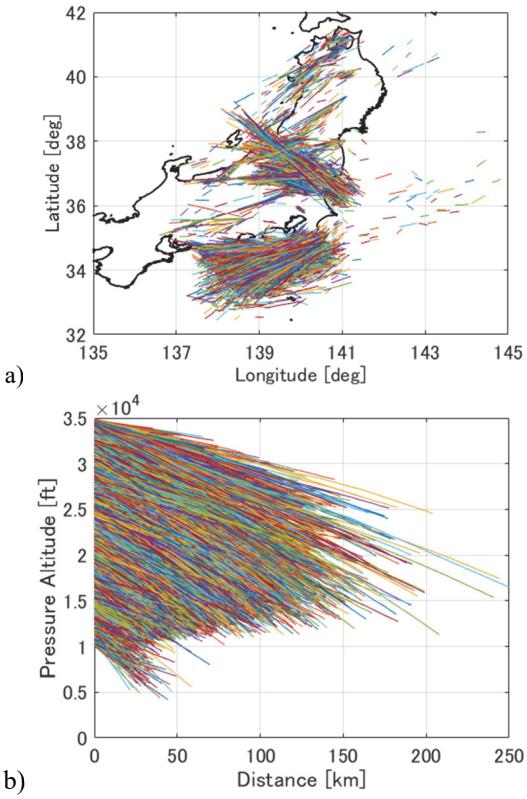

Figure 1. Extracted trajectories (N = 80,543), a: horizontal, and b: vertical.

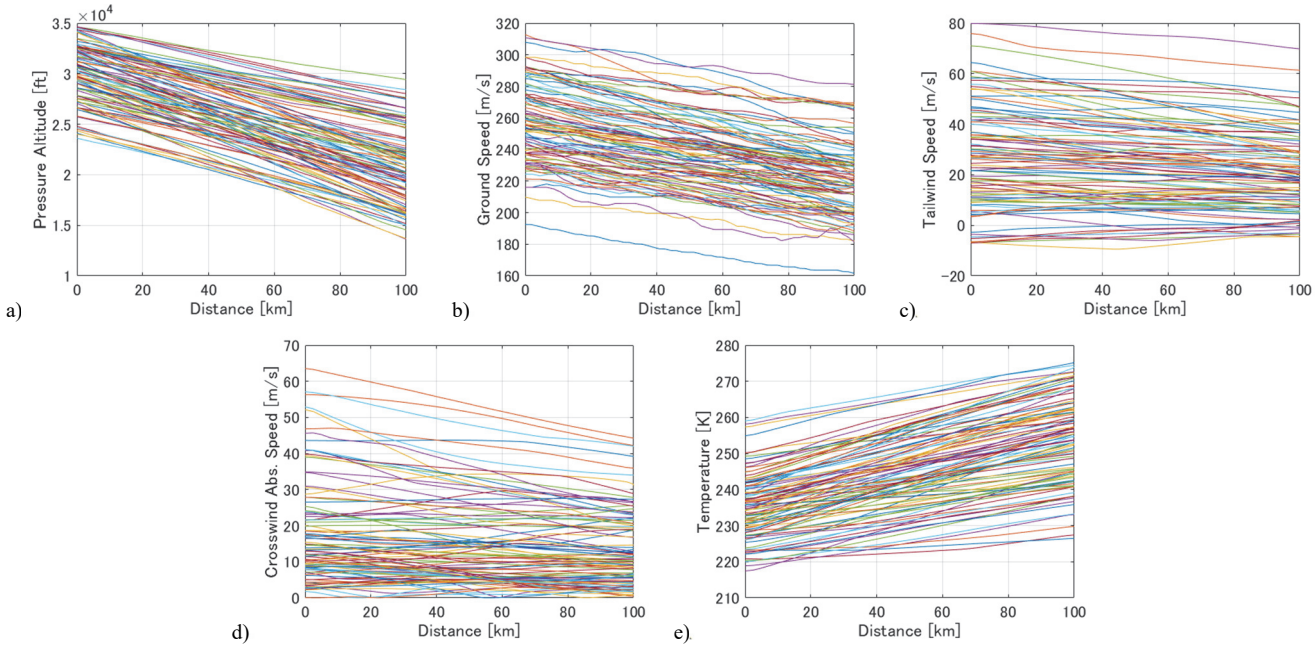

Figure 2. Example trajectories (N = 100), a: pressure altitude, b: GS, c: tailwind speed, d: absolute value of crosswind speed, and e: temperature.

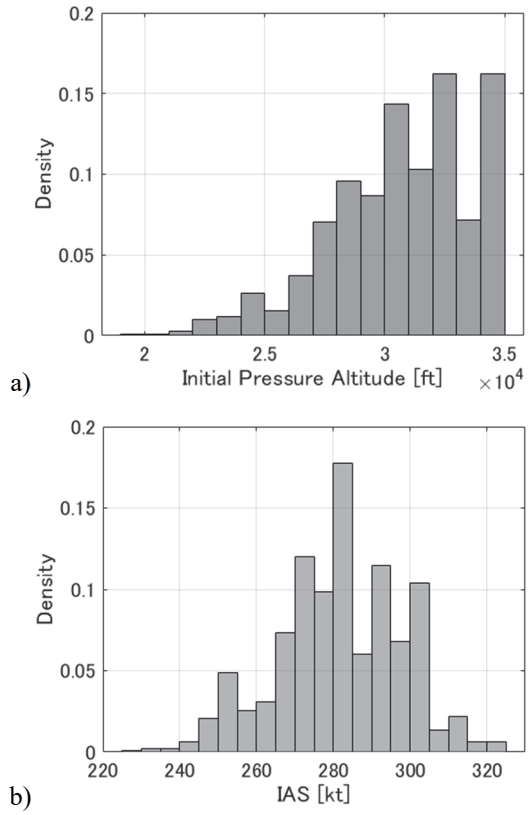

Figure 3. Histograms of a: initial altitude and b: mean IAS (N = 1108).

III. Modeling of Flight Time Uncertainty

A. Flight-Time Prediction Error Calculation

The first step is to calculate the flight-time prediction error at a distance of 100 km. In this study, it is assumed that each flight keeps the IAS constant at the value indicated by the ATCOs, while keeping the FPA constant so that the flight will be at the same altitude as the actual trajectory at a distance of 100 km. The ATCOs are assumed to indicate the IAS every 10 kt and the value of the intended IAS is obtained by rounding the average IAS values of the actual trajectory to the nearest 10 kt. To obtain the GS of the predicted trajectory, the intended IAS is first converted to TAS according to the following formula [27] using the weather forecast value:

$$V_{TAS,int} \coloneqq V_{TAS}\left(V_{IAS,int},T\right) = \sqrt{\frac{2}{\mu}RT\left(\left(1+\frac{p_0}{p}\left(\left(1+\frac{\mu}{2}\frac{\rho_0}{p_0}V_{IAS,int}\right)^{\frac{1}{\mu}}-1\right)\right)^{\mu}-1\right)}. \quad (1)$$

This conversion is a function of IAS and temperature. The geometric relationship among the converted TAS and the TAS in the flight direction, crosswind, tailwind, and GS is shown in Fig 4. Using the crosswind value obtained from the numerical weather forecast, the component of TAS in the flight direction is obtained and the tailwind is added to obtain the intended GS as follows:

$$V_{GS,int} = V_{TAStr} + W_t = \sqrt{V_{TAS}^2\left(V_{IAS,int},T\right) - W_c^2} + W_t. \quad (2)$$

The predicted time to reach D=100 km is obtained by integrating the intended GS:

$$\int_0^{t_{pred}} V_{GS,int}\,dt = D. \quad (3)$$

The actual flight time is also obtained by integrating the actual GS:

$$\int_0^{t_{act}} V_{GS,act}\,dt = D. \quad (4)$$

The flight-time prediction error is defined as the difference between these values:

$$t_{err} \coloneqq t_{act} - t_{pred}. \quad (5)$$

In this study, trajectories up to a distance of 100 km were analyzed using the fourth-order Runge–Kutta method. A plot of flight-time prediction errors for the 1108 trajectories is shown in Fig. 5. A histogram of flight-time prediction errors at a distance of 100 km is shown in Fig. 6. The mean error (ME) and STD of the prediction error were −1.64 s and 3.77 s, respectively. Plots of the ME, STD, and root mean squared error (RMS) of the flight-time prediction error are shown in Fig. 7. The ME is considered to be caused by some systematic errors in weather forecasts and aircraft controls and can be eliminated when sufficient data is available. On the other hand, variability is thought to be caused by variations in atmospheric conditions and aircraft control, and is considered to be unpredictable. Therefore, hereinafter, this study focuses on the prediction of the magnitude of the variance and standard deviation of the flight-time prediction error.

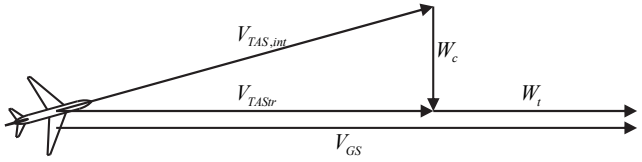

Figure 4. Geometric relationship of aircraft GS, TAS, and wind speed.

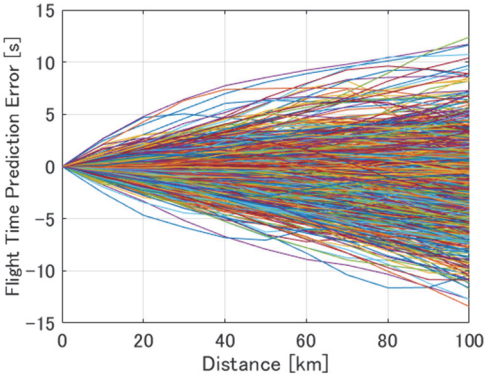

Figure 5. Flight-time prediction errors (N = 1108).

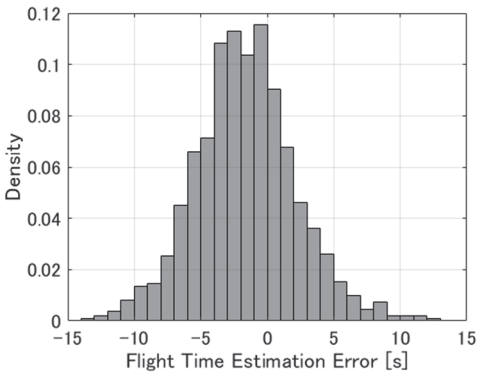

Figure 6. Histogram of flight-time prediction errors at 100 km (N = 1108).

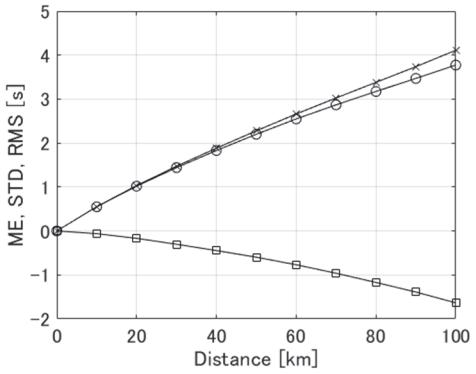

Figure 7. Plots of ME (squares), STD (circles), and RMS (crosses) of flight-time prediction error (N = 1108).

B. Theoretical Basis

Next, a theoretical description of the flight-time prediction uncertainty for trajectories where flight and atmospheric conditions vary is derived. The predicted flight-time for a given *i*-th small interval is given by:

$$\Delta T_i + t_i = \frac{\Delta D_i}{V_{GS,i} + v_i}, \tag{6}$$

where $V_{GS,i}$ is intended GS, ΔT_i is exact flight time, t_i is the flight-time prediction error, and v_i is GS deviation. The flight-time prediction error in this interval is given by:

$$t_i = -\frac{\Delta D_i}{V_{GS,i}^2} v_i . \tag{7}$$

From this, the variance of the flight-time prediction error that arises in the small interval is given by [28]:

$$\sigma_{t_i}^2 = \frac{\Delta D_i^2}{V_{GS,i}^4} \sigma_{v_i}^2 . \tag{8}$$

The deviations in GS are described by:

$$v_i = v_{i-1} + e_i = e_1 + e_2 \cdots + e_i . \tag{9}$$

where e_i is GS fluctuation. This is equivalent to modeling the GS deviation as a random walk process. The variance of the GS deviation is obtained with:

$$\sigma_{v_i}^2 = \left\langle \left(e_1 + e_2 \cdots + e_i\right)^2 \right\rangle = \left\langle e_1^2 + e_2^2 \cdots + e_i^2 \right\rangle = \sum_{j=1}^{i} \sigma_{e_j}^2 . \tag{10}$$

Here, it is assumed that the fluctuations occurring in each small interval are independent of each other. Then, the variance of the flight-time prediction error occurring in this small interval $\sigma_{t_i}^2$ is obtained as follows:

$$\sigma_{t_i}^2 = \frac{\Delta D_i^2}{V_{GS,i}^4} \sum_{j=1}^{i} \sigma_{e_j}^2 . \tag{11}$$

From this, the variance of the flight-time prediction error to a desired flight distance σ_T^2 can be expressed as:

$$\sigma_T^2 = \sum_{i=1}^{n} \sigma_{t_i}^2 = \sum_{i=1}^{n} \left(\frac{\Delta D_i^2}{V_{GS,i}^4} \sum_{j=1}^{i} \sigma_{e_j}^2 \right). \tag{12}$$

In the next section, the validity of this prediction method will be examined by analyzing actual data.

C. Modeling of Short Segment Data

In the previous section, it was shown that the flight-time prediction uncertainty of a descent trajectory can be modeled using the uncertainty of small intervals. Therefore, using the large amount of trajectory data obtained in this study for trajectories of less than 100 km, a model of the relationship between flight and atmospheric conditions and the flight time prediction uncertainty in short segments is constructed. The feasibility of flight-time uncertainty prediction for trajectories of 100 km using this model is investigated in the next section.

First, the predicted and actual flight times, and average values of wind speed and temperature for the initial 10 km section of each trajectory are obtained, assuming that the variation of atmospheric conditions is negligible in the 10 km section. The intended IAS values of each trajectory are also obtained by rounding off the average IAS to the nearest 10 kt. Histograms of initial altitude, mean IAS, intended IAS, mean tailwind, absolute value of mean crosswind, and mean temperature for 79,435 trajectories are shown in Fig. 8. From these distributions, it is confirmed that the ranges of initial altitude and intended IAS of the 10 km trajectory data and the atmospheric conditions are sufficient to include those of the 100 km trajectories shown in Figures 2 and 3. A histogram of the flight-time prediction error is shown in Fig. 9. From this, it can be confirmed that the distribution is almost close to the normal distribution, with a slight bias. The ME was 1.7×10^{-3} s, and the STD was 0.51 s.

Next, the equation relating flight and atmospheric conditions and flight-time prediction error is derived. The flight time for a small interval can be described as follows:

$$\Delta T = \frac{\Delta D}{\sqrt{V_{TAS}^2\left(V_{IAS},T\right) - W_c^2} + W_t}. \quad (13)$$

The equation relating wind speed, temperature, and intended IAS to variance of the flight-time prediction error is obtained through the law of uncertainty propagation [28]. The following equation is obtained from the total derivatives of both sides:

$$\begin{aligned} t_i &= \frac{\partial f}{\partial W_t}dW_t + \frac{\partial f}{\partial W_c}dW_c + \frac{\partial f}{\partial T}dT + \frac{\partial f}{\partial V_{IAS}}dV_{IAS} \\ &= -\frac{\Delta D_i}{V_{GS}^2}dW_t + \frac{\Delta D_i}{V_{GS}^2}\frac{W_c}{V_{TAStr}}dW_c \\ &\quad -\frac{\Delta D_i}{V_{GS}^2}\frac{V_{TAS}}{V_{TAStr}}\frac{\partial V_{TAS}}{\partial T}dT - \frac{\Delta D_i}{V_{GS}^2}\frac{V_{TAS}}{V_{TAStr}}\frac{\partial V_{TAS}}{\partial V_{IAS}}dV_{IAS} \end{aligned}. \quad (14)$$

The variance of the flight-time prediction error is obtained as a function of wind, temperature, and IAS and their fluctuations:

$$\begin{aligned} \sigma_t^2 &= \frac{\Delta D^2}{V_{GS}^4}\left(1+\left(\frac{W_c}{V_{TAStr}}\right)^2\right)\sigma_W^2 \\ &+ \frac{\Delta D^2}{V_{GS}^4}\left(\frac{V_{TAS}}{V_{TAStr}}\frac{\partial V_{TAS}}{\partial T}\right)^2\sigma_T^2 + \frac{\Delta D^2}{V_{GS}^4}\left(\frac{V_{TAS}}{V_{TAStr}}\frac{\partial V_{TAS}}{\partial V_{IAS}}\right)^2\sigma_{V_{IAS}}^2 \end{aligned}. \quad (15)$$

where the variance of the tailwind and crosswind is considered equal, and W, T, and IAS are assumed to be independent of each other. Since the variance values correspond to errors in weather forecasts and flight-speed control of the aircraft, and cannot be predicted in advance, they are treated here as coefficients:

$$\begin{aligned} \sigma_t^2 &= \alpha_W \frac{\Delta D^2}{V_{GS}^4}\left(1+\left(\frac{W_c}{V_{TAStr}}\right)^2\right) \\ &+ \alpha_T \frac{\Delta D^2}{V_{GS}^4}\left(\frac{V_{TAS}}{V_{TAStr}}\frac{\partial V_{TAS}}{\partial T}\right)^2 + \alpha_V \frac{\Delta D^2}{V_{GS}^4}\left(\frac{V_{TAS}}{V_{TAStr}}\frac{\partial V_{TAS}}{\partial V_{IAS}}\right)^2 \end{aligned}. \quad (16)$$

This is further simplified by introducing x:

$$\sigma_t^2 = \alpha_W x_W + \alpha_T x_T + \alpha_V x_V, \quad (17)$$

where:

$$\begin{aligned} x_W &:= \frac{\Delta D^2}{V_{GS}^4}\left(1+\left(\frac{W_c}{V_{TAStr}}\right)^2\right), x_T := \frac{\Delta D^2}{V_{GS}^4}\left(\frac{V_{TAS}}{V_{TAStr}}\frac{\partial V_{TAS}}{\partial T}\right)^2, \\ x_V &:= \frac{\Delta D^2}{V_{GS}^4}\left(\frac{V_{TAS}}{V_{TAStr}}\frac{\partial V_{TAS}}{\partial V_{IAS}}\right)^2 \end{aligned}. \quad (18)$$

Then, in order to appropriately determine the variance of the flight-time prediction error and the values of α, it is necessary to collect a large amount of similar data. To this end, in this study, k-means clustering [29] is applied. The feature vector for clustering is defined as follows:

$$\mathbf{y}_i := \left(x_{W,i}, x_{T,i}, x_{V,i}\right)^T. \quad (19)$$

where $x_{W,i}$, $x_{T,i}$ and $x_{V,i}$ are calculated applying the average values of parameters for each trajectory. Since each cluster must have a sufficient number of samples in order to obtain accurate statistics, clusters with less than a threshold number of samples k_{Thre} are excluded from the analysis. The following steps are used to perform the regression analysis: 1) determine the variance of the flight-time prediction error and the mean values of x for each cluster with a sufficient number of samples; 2) apply principal component analysis (PCA) [29] to the feature vectors and extract the eigenvectors that primarily explain the variances; 3) determine the coefficients of Eq. (17) via multiple regression analysis; 4) estimate the variances of all samples using the regression equation; 5) normalize the flight-time prediction error of all samples via the estimated variance and calculate their STD. To determine the appropriate numbers of the initial clusters k_{ini} and threshold k_{Thre}, a grid search was carried out for k_{ini} = 10, 30, 100, and k_{Thre} = 100, 300, 1000, and results clarified that no clusters were excluded and the calculated STD became closest to 1 for k_{ini} = 10.

The PCA reveals that 99.9% of the variance can be explained by the principal vectors alone. This is presumable because there are strong correlations between each of the x parameters. The result of the regression analysis is obtained as:

$$\begin{aligned} \sigma_t^2[s^2] &= \frac{\Delta D^2}{V_{GS}^4}\sigma_e^2 \\ &= 0.11x_W + 0.14x_T + 0.54x_V + 0.17 \end{aligned}. \quad (20)$$

The adjusted $R^2 = 0.97$, with p-values < 0.01 for all parameters. The constant term that appears in this equation is thought to correspond to the unavoidable fluctuations in wind, temperature and aircraft speed control. This equation gives the variance of the flight time prediction error at a distance of 10 km from the speed and atmospheric conditions.

To investigate the validity of this model, all of the 10 km trajectory data are classified into four clusters by k-means clustering according to the estimated value of variance. These clusters can be interpreted as severe, normal, and calm clusters in the order of their predicted values of variance. The flight-time prediction error of each trajectory within each cluster is normalized by the estimated STD. The results are compared with the case of normalizing by the STD of the overall flight-time prediction error. The results are summarized in Fig.10. It can be seen that, in the case of normalization by the overall STD, the STD values of prediction error are overestimated in calm conditions and underestimated in severe conditions. In contrast, when normalized by the predicted STD, the STD values of the normalized error are almost equal to 1 in all cases. Therefore, it can be concluded that this model accurately predicts the flight-time prediction uncertainty for 10 km trajectories.

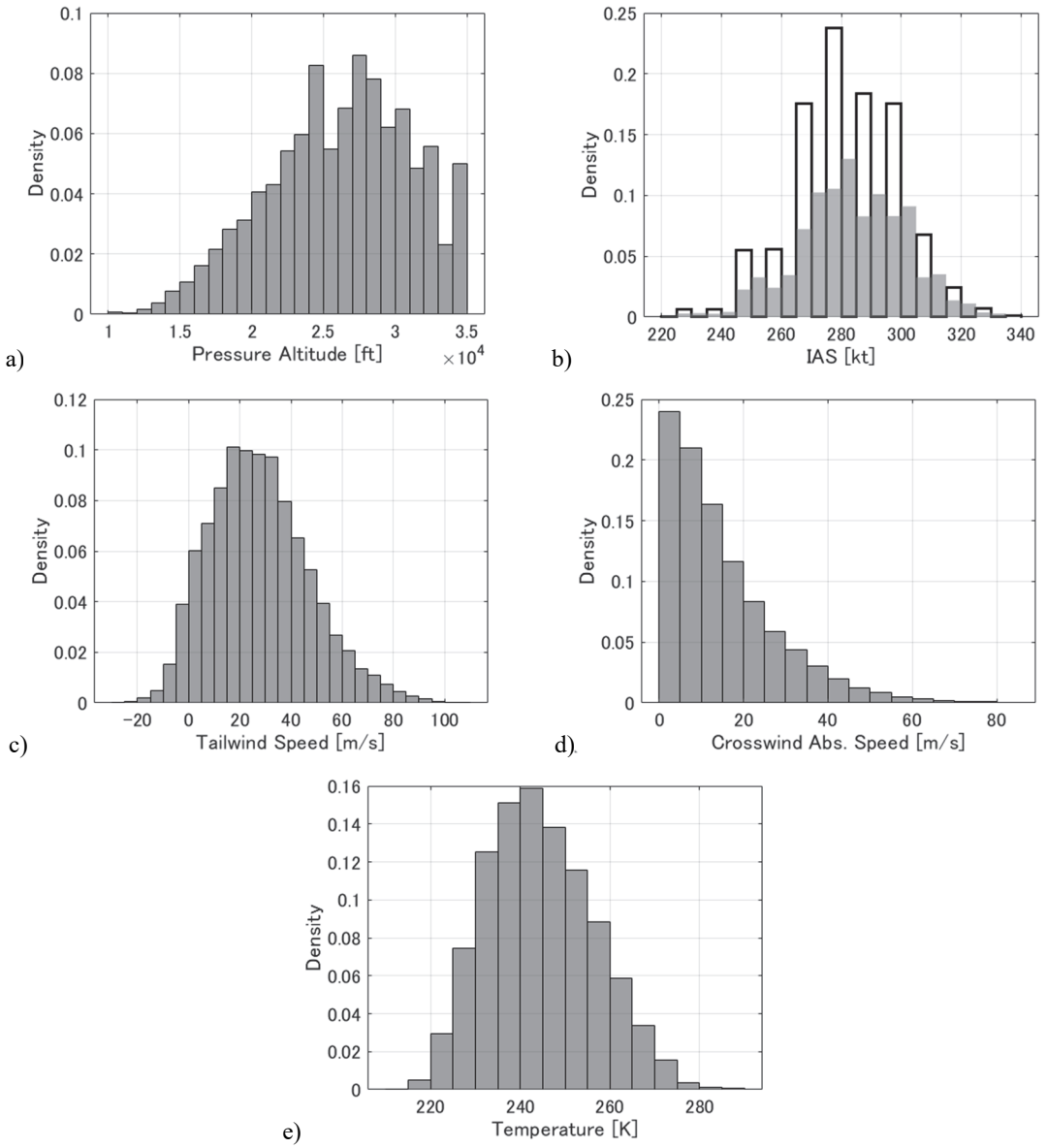

Figure 8. Histograms of a: initial altitude, b: mean (gray) and intended (white) IAS, c: tailwind speed, d: absolute values of crosswind speed, and e: temperature (N = 79,435).

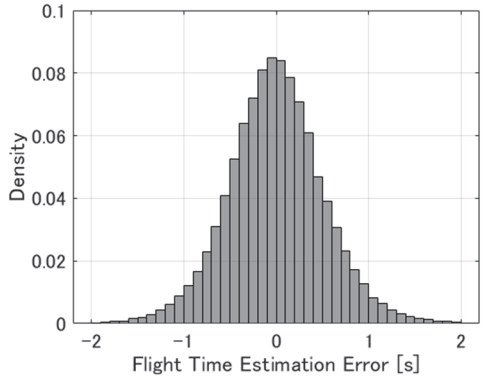

Figure 9. Histograms of flight-time prediction error (N = 79,435).

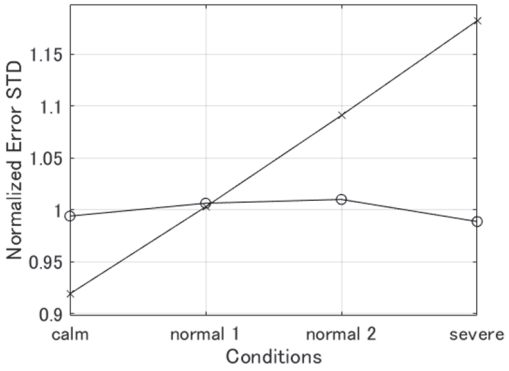

Figure 10. STD of prediction error normalized by predicted STD (circles) and overall STD (crosses)

D. Uncertainty Modeling in Descent Trajectories

In this chapter, the modeling of the flight-time prediction uncertainty at a distance of 100 km in the descent trajectory is evaluated. From Eq. (11), the increase in variance can be predicted from the atmospheric conditions and the intended IAS in small intervals. Through the summation in Eq. (12), it should be possible to obtain the flight-time prediction uncertainty at a flight distance of 100 km. For this purpose, each trajectory is first divided into short segments of 10 km each. Then, by substituting the intended IAS and the average values of atmospheric conditions of the short segment into Eq. (18) and (20), and substituting the values into Eq. (11), the increase of variance in the segment is obtained. Finally, by summation according to Eq. (12), the variance of flight time prediction error for the entire trajectory can be obtained.

The predicted and actual STD for all trajectories are summarized in Fig. 11. It can be confirmed that the proposed method is able to approximately predict the STD values of actual trajectories. This result also indicates that improvements are still possible in the modeling. The normalized error $\Delta T_{nom,i}$ can be obtained by dividing the flight-time prediction error $\Delta T_{pred,i}$ minus the average error ΔT_{mean} by the predicted STD $\sigma_{T,i}$:

$$\Delta T_{nom,i} = \frac{\Delta T_{pred,i} - \Delta T_{mean}}{\sigma_{T,i}} . \tag{21}$$

The histogram and normal probability plot at a flight distance of 100 km are shown in Figures 12 and 13, respectively. The distribution of the normalized error is almost the same as the standard normal distribution.

The next step is to investigate the feasibility of accurately predicting the change of flight-time prediction uncertainty due to flight and atmospheric conditions. For this purpose, *k*-means clustering is applied using the predicted STD at a distance of 100 km as the feature parameter. The results are summarized in Fig. 14, where the prediction errors normalized by the predicted STD and by the overall STD are compared. The results show that the STD normalized by the overall STD becomes smaller than 1 in calm conditions and greater than 1 in severe conditions. These correspond to overestimation and underestimation, respectively. On the other hand, the STD normalized by the predicted STD become almost equal regardless of the condition, although it slightly deviates from 1 overall. This result indicates that it is still possible to predict whether the condition becomes severe or calm, even though the overall situation is slightly overestimated.

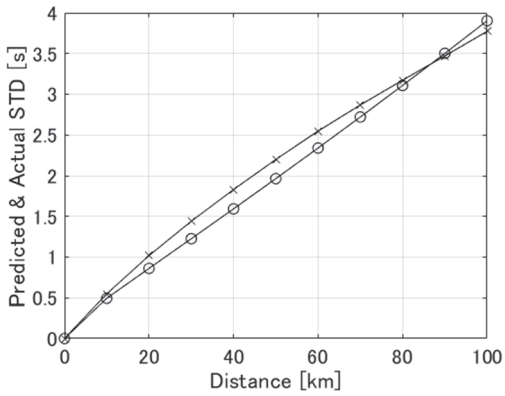

Figure 11. Plot of predicted (circles) and Actual (crosses) STD (N = 1108).

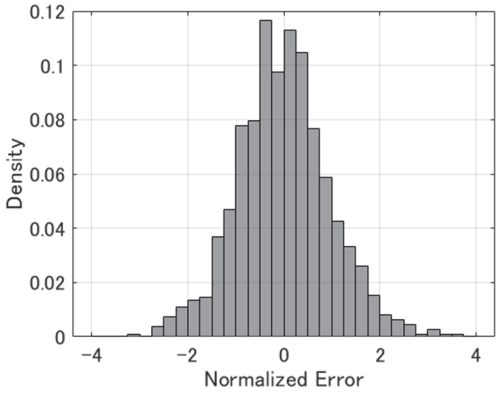

Figure 12. Histograms of flight-time prediction error normalized by predicted STD at 100 km (N = 1108).

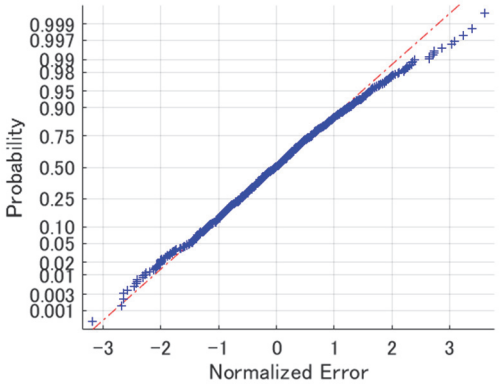

Figure 13. Normal probability plot of flight-time prediction error normalized by predicted STD at 100 km (N = 1108).

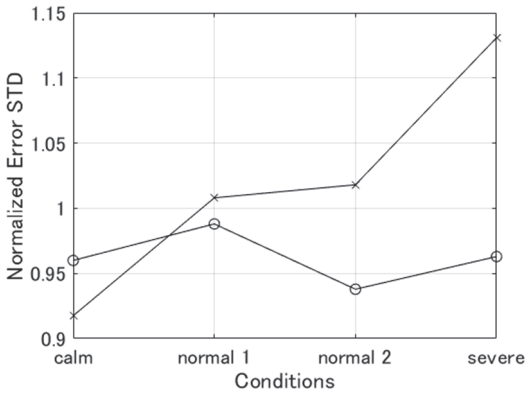

Figure 14.STD of prediction error normalized by predicted STD (circles) and overall STD (crosses) of descent trajectories at 100 km (N = 1108).

IV. CONCLUSION

A flight-time prediction uncertainty model that takes into account changes in flight and atmospheric conditions in the descent trajectory was derived theoretically by modeling the flight speed fluctuation as a random walk process. The relationship between the flight-time prediction uncertainty and the flight and atmospheric conditions was determined by analyzing a large amount of short segments of data. By applying this relationship, it is clearly demonstrated that the flight-time prediction uncertainty of the descent trajectory can be predicted approximately accurately. This prediction model will enable accurate prediction of potential magnitude of post-descent deviation of the flight-time before initiating the descent using numerical weather forecast data. This will improve the efficiency of the management of four-dimensional descent trajectory to congested airports without compromising the safety.

In this study, a theoretical flight-time prediction uncertainty model was developed based on a flight dynamics model that, through the strict use of necessary and sufficient parameters including weather conditions, gives accurate estimates of flight time. On the other hand, several previous studies have shown that machine learning can also be used to predict flight time and its uncertainty using parameters that are difficult to treat analytically, such as traffic conditions. Even with such machine learning techniques, however, further improvement in accuracy is expected by introducing the theory-based model presented in this study as one of the feature parameters.

One future work is to clarify an air-traffic management strategy that utilizes the proposed flight-time prediction uncertainty model. It is possible to extend the proposed methodology to flight-time uncertainty prediction for trajectories with multiple segments. Once this becomes possible, it can be used to predict flight-time uncertainty in arbitrary situations, and will contribute to various types of four-dimensional trajectory management in the future.

REFERENCES

[1] Civil Aviation Bureau of the Ministry of Land, Infrastructure, Transport and Tourism, “Collaborative Actions for Renovation of Air Traffic Systems,” https://www.mlit.go.jp/en/koku/koku_fr13_000029.html (cited Apr. 18, 2021)

[2] Federal Aviation Administration, “Vision for Trajectory Based Operations,” Tech. rep., Washington, DC, 2017. https://www.faa.gov/air_traffic/technology/tbo/documents/ (cited Apr. 18, 2021)

[3] R. A. Paielli and H. Erzberger, “Conflict Probability Estimation for Free Flight,” Journal of Guidance, Control, and Dynamics, Vol. 20, No. 3, 1997, pp. 588-596.

[4] D. B. Nicholls, P. Battino, P. Marti and S. Pozzi, “Presenting Uncertainty to Controllers and Pilots,” Proceedings of the 5th USA/Europe Air Traffic Management Research and Development Seminar, Budapest, Jun. 23-27, 2003.

[5] D. Schaefer, A. Gizdavu, and D. B. Nicholls, “The Display of Uncertainty Information on the Working Position,” 23rd IEEE/AIAA Digital Avionics Systems Conference, Washington D.C., Oct. 2004.

[6] M. Tielrooij, C. Borst, D. Nieuwenhuisen, M. Mulder and D. Schaefer, “Supporting Arrival Management Decisions by Visualising Uncertainty,” Proceedings of the SESAR Innovation Days, Stockholm, Sweden, 2013.

[7] J. Thipphavong, and D. Mulfinger, “Design Considerations for a New Terminal Area Arrival Scheduler,” AIAA Aviation Technology, Integration, and Operations Conference, AIAA Paper 2010-9290, Sept. 2010.

[8] S. Shresta, and R. H. Mayer, “Benefits and Constraints of Time-Based Metering Along RNAV STAR Routes,” 28th IEEE/AIAA Digital Avionics Systems Conference, IEEE Publ., Piscataway, NJ, Oct. 2009, pp. 2.B.3-1-10. https://doi.org/10.1109/DASC.2009.5347549

[9] I. M. Levitt, L. A. Weitz, and M. W. Castle, “Modeling Delivery Accu racy for Metering Operations to Support RNAV Arrivals,” 10th USA/Europe Air Traffic Management Research and Development Seminar, Chicago, IL, June 2013,

http://atmseminar.org/seminarContent/seminar10/papers/255-Levitt_0127130117-Final-Paper-4-15-13.pdf.

[10] L. A. Weitz, B. J. Lascara, and R. M. Sgorcea, “Deriving Estimated Time of Arrival Accuracy Requirements for Time-Based Traffic Management,” Proceedings of the AIAA Science and Technology Forum, 2020.

[11] S. Förster, M. Schultz and H. Fricke, “Probabilistic Prediction of Separation Buffer to Compensate for the Closing Effect on Final Approach,” Aerospace, Vol. 8, No. 29, 2021.

[12] R. Irvine, “A Geometrical Approach to Conflict Probability Estimation,” Air Traffic Control Quarterly, Vol. 10, No. 2, 2002, pp. 85–113. https://doi.org/10.2514/atcq.10.2.85

[13] R. A. Paielli, “Empirical Test of Conflict Probability Estimation,” 2nd USA/Europe Air Traffic Management Research and Development Seminar, Orlando, FL, Dec. 1998,

http://atmseminar.org/seminarContent/seminar2/papers/p_010_SMIAO.pdf.

[14] E. Robert, and D. De Smedt, “Comparison of Operational Wind Forecasts with Recorded Flight Data,” 10th USA/Europe Air Traffic Management Research and Development Seminar, Chicago, IL, June 2013, http://atmseminar.org/seminarContent/seminar10/papers/211-ROBERT_0125131206-Final-Paper-4-10-13.pdf.

[15] T. L. Gaydos, W. Kirkman, W. Shresta, E. Blair, and J. Kuchenbrod, “Measured Variability and Uncertainty in Flight Operations,” IEEE Integrated Communications, Navigation and Surveillance Conference, IEEE Publ., Piscataway, NJ, April 2012.

[16] M. Tielrooij, C. Borst, M. M. Van Paassen and M. Mulder, “Predicting Arrival Time Uncertainty from Actual Flight Information,” Proceedings of the 11th USA/Europe Air Traffic Management Research and Development Seminar, Lisbon, Jun. 23-26, 2015.

[17] A. Franco, D. Rivas, and A. Valenzuela, “Probabilistic Aircraft Trajectory Prediction in Cruise Flight Considering Ensemble Wind Forecasts,” Aerospace Science and Technology, Vols. 82–83, Nov. 2018, pp. 350–362. https://doi.org/10.1016/j.ast.2018.09.020

[18] D. González-Arribas, M. Soler, and M. Sanjrujo, “Robust Aircraft Trajectory Planning Under Wind Uncertainty Using Optimal Control,” Journal of Guidance, Control, and Dynamics, Vol. 41, No. 3, 2018, pp. 673–688. https://doi.org/10.2514/1.G002928

[19] A. Franco, D. Rivas, and A. Valenzuela, “Optimal Aircraft Path Planning in a Structured Airspace Using Ensemble Weather Forecasts,” 8th

SESAR Innovation Days, Salzburg, Austria, Dec. 2018. https://www.sesarju.eu/sites/default/files/documents/sid/2018/papers/SIDs_2018_paper_55.pdf.

[20] D. Rivas, R. Vazquez, and A. Franco, "Stochastic Analysis of Fuel Consumption in Aircraft Cruise Subject to Along-TrackWind Uncertainty," Aerospace Science and Technology, Vol. 66, July 2017, pp. 304–314. https://doi.org/10.1016/j.ast.2017.03.027

[21] N. Takeichi, "Adaptive Prediction of Flight Time Uncertainty for Ground-Based 4-D TrajectoryManagement," Transportation Research, Part C, Emerging Technologies, Vol. 95, Oct. 2018, pp. 335–345. https://doi.org/10.1016/j.trc.2018.07.028

[22] N. Takeichi, T. Yamada, A. Senoguchi, and T. Koga, "Development of a Flight Time Uncertainty Model for Four-Dimensional Trajectory Management," Journal of Air Transportation, Vol. 28, No. 3, Jul.-Sept. 2020, pp. 134–143.

[23] H. Paek, K. Lee and A. E. Vela, "En-route Arrival Time Prediction using Gaussian Mixture Model," The 9th International Conference for Research in Air Transportation, Online, Sep. 15, 2020.

[24] I. Dhief, Z. Wang, M. Liang, S. Alam, M. Schultz, and D. Delahaye, "Predicting aircraft landing time in extended-tma using machine learning methods," The 9th International Conference for Research in Air Transportation, Online, Sep. 15, 2020.

[25] A. Senoguchi and T. Koga, "Analysis of Downlink Aircraft Parameters Monitored by SSR Mode S in ENRI," 28th Digital Avionics Systems Conference, Orlando, Florida, Oct. 25-29, 2009.

[26] Japan Meteorological Agency, "Numerical Weather Prediction Activities," https://www.jma.go.jp/jma/en/Activities/nwp.html (cited Apr. 15, 2021)

[27] A. Nuic, "User Manual for the Base of Aircraft Data (BADA) Revision 3.11," EUROCONTROL, Brussels, 2013.

[28] H. J. Berendsen, "A student's guide to data and error analysis," Cambridge University Press, 2011.

[29] T. Hastie, R. Tibshirani and J. Friedman, "The Elements of Statistical Learning: Data Mining, Inference, and Prediction, Second Edition," Springer, 2009.

Noboru Takeichi is a professor at the Department of Aeronautics and Astronautics at Tokyo Metropolitan University. He received B.E., M.E., and Ph.D. degrees in Engineering from the University of Tokyo in 1997, 1999, and 2002, respectively. After working for the Japan Aerospace Exploration Agency and the Electronic Navigation Research Institute as a researcher, he joined the Department of Aerospace Engineering at Nagoya University as an associate professor in 2008, then moved to Tokyo Metropolitan University in 2015. His research interests include air traffic management, UAS traffic management and space traffic management such as operations of space debris removal systems.

Ryota Hashimoto is a graduate student at the Department of Aeronautics and Astronautics at Tokyo Metropolitan University. He received B.E. in Engineering from Tokyo Metropolitan University in 2020.